

Improving Emotion Recognition from Ambiguous Speech via Spatio-Temporal Spectrum Analysis and Real-Time Soft-Label Correction

Chenquan Gan, Daitao Zhou, Qingyi Zhu, *Member, IEEE*, Xibin Wang, *Member, IEEE*, Deepak Kumar Jain, *Senior Member, IEEE*, and ^{*}Vitomir Štruc, *Senior Member, IEEE*

Abstract—Speech represents a fundamental medium for conveying human emotions and, as a result, speech-based emotion recognition (SER) systems have become pivotal in advancing human-computer interaction (HCI) across a range of applications. While significant progress has been made in speech emotion recognition over recent years, existing solutions still face several key challenges, in that they: (i) rely excessively on subjectively annotated (discrete) labels during training, (ii) often overlook the label ambiguity of speech samples that express more than one class of emotions, and (iii) underutilize unlabeled or ambiguous speech, for which typically a label distribution (or so-called soft labels) is available. To address these issues, we propose in this paper a novel SER model that explicitly handles ambiguous speech samples and overcomes the shortcomings outlined above. Central to our approach is a novel real-time soft-label correction strategy designed to refine the annotations assigned to ambiguous speech. The proposed model leverages both, (explicitly) labeled as well as ambiguous samples and applies the dynamic soft-label correction strategy alongside an enhanced inter-class difference loss function to iteratively optimize the label distributions during training. We theoretically demonstrate that our method is capable of approximating the true emotional distribution of speech even in the presence of label noise, suggesting that utilizing ambiguous speech samples without explicit emotion labels still contributes toward more effective emotion recognition. Furthermore, we integrate the representational power of convolutional neural networks (CNNs) with the contextual modeling capabilities of Wav2Vec 2.0 to enable a comprehensive extraction of spatio-temporal speech features. Experimental results on the IEMOCAP multi-label dataset confirm the effectiveness of our approach, achieving state-of-the-art performance with significant improvements in weighted accuracy (WA) and unweighted accuracy (UA) over competing methods.

Index Terms—Speech emotion recognition, ambiguous speech, soft labels, real-time correction, spatio-temporal analysis

I. INTRODUCTION

Speech is one of the most natural ways of human communication that can directly express intentions and even emotional states. The process of using computer technology to analyze sound features from speech signals and infer the speaker's emotional state is commonly referred to as *speech emotion recognition* (SER) [1]–[3]. Speech emotion recognition has transitioned from a specialized research area to a significant component of human-computer interaction (HCI) [4], capable of enhancing user experience in various application domains [5], ranging from call-center conversations and in-vehicle vehicle driving systems to smart-home application and smart healthcare among others [6].

Currently, most speech emotion recognition methods mainly rely on explicit (hard) labels for model training [7], [8], where each speech sample is assigned a single, discrete emotion category. While such methods have achieved notable success, they fall short in capturing the complexity of emotional expression in real-world scenarios, where speech often conveys multiple overlapping emotions. For instance, an utterance labeled as "sad" may concurrently also convey feelings of anger and disappointment [9]. This illustrates the inherent ambiguity and subjectivity present in emotional expression through speech [10]. Moreover, emotional perception in speech can also vary significantly across annotators due to individual differences in cultural background, gender, age, and other similar factors, suggesting that emotion perception is inherently subjective [11]. Consequently, SER methods that rely on single-label annotations not only fail to account for the ambiguity in emotional expression but also overlook the impact of subjective cognitive biases among annotators, which is one of the primary sources of label noise in emotion datasets [12].

To address the limitations of single-label annotation, recent research has increasingly explored multi-label approaches for speech emotion recognition [13], [14]. Multi-labeled methods leverage sets of emotion categories identified by multiple annotators to represent the presence of various emotions within a single utterance. While such approaches better capture the multifaceted nature of emotional expression, they still fall short in modeling the relative prominence of each emotion. In practice, speech often conveys a mixture of emotions, with one dominant emotion prevailing within the overall mixture. Traditional multi-label techniques are typically unable to represent these proportions effectively. To mitigate this issue, researchers

^{*}Corresponding author

This work is supported by the Guangxi Key Research and Development Program (No. AB24010317).

C. Gan and D. Zhou are with School of Communications and Information Engineering, Chongqing University of Posts and Telecommunications, Chongqing 400065, China (e-mail: gcq2010cqu@163.com; s220101216@stu.cqupt.edu.cn).

Q. Zhu is with School of Cyber Security and Information Law, Chongqing University of Posts and Telecommunications, Chongqing 400065, China (e-mail: zhuqy@cqupt.edu.cn).

X. Wang is with College of Data Science, Guizhou Institute of Technology, Guiyang 550025, Guizhou, China (e-mail: binxiwang@git.edu.cn)

D. Jain is with the Key Laboratory of Intelligent Control and Optimization for Industrial Equipment of the Ministry of Education, Dalian University of Technology, Dalian 116024, China (e-mail: dkj@ieee.org).

V. Štruc is with Faculty of Electrical Engineering, University of Ljubljana, Tržaska cesta 25, SI-1000 Ljubljana (e-mail: vitomir.struc@fe.uni-lj.si).

80 have introduced soft-label strategies [15], [16], where the
 81 distribution of annotator votes is used to assign weights to
 82 each emotion category, offering a more nuanced description of
 83 emotional content of the analyzed speech samples. However,
 84 such a soft-label approaches still heavily rely on the subjective
 85 judgments of a limited pool of annotators, and as a result,
 86 may introduce significant statistical noise and inconsistencies,
 87 which pose a considerable challenge for reliable training of
 88 speech emotion recognition (SER) models.

89 Furthermore, several studies have investigated the use of
 90 ambiguous speech samples for emotion recognition through
 91 multi-classifier interaction learning [17] and joint-learning
 92 frameworks in an attempt to mitigate the limitations
 93 of multiple and soft labels by allowing the model to infer
 94 emotional distributions directly from the data. However, such
 95 approaches typically overlook speech samples that lack dom-
 96 inant emotions, i.e., samples that inherently carry the most
 97 ambiguity. In practice, the subjectivity of emotion perception
 98 and the ambiguity of emotional expression are most evident in
 99 these unlabeled or weakly labeled instances, where annotators
 100 are less likely to agree on a dominant emotion due to unclear
 101 affective cues [19]. This leads to inconsistencies in annotations
 102 and challenges in model training. Moreover, in real-world
 103 scenarios, it is common for speech utterances to lack a clearly
 104 dominant emotion that is agreed upon by a majority of
 105 annotators. As a result, existing methods that depend solely
 106 on speech samples with consensus labels fail to capture the
 107 full complexity of emotional ambiguity and do not adequately
 108 address the inherent uncertainty present in natural speech.

109 To address the above challenges, we propose in this paper
 110 a novel model for speech emotion recognition that explicitly
 111 targets the inherent uncertainty and ambiguities in emotional
 112 speech. Our approach simultaneously incorporates both un-
 113 labeled examples as well as samples with explicit discrete
 114 labels during training. Labeled samples provide supervision
 115 to guide the learning process, while ambiguous samples
 116 are iteratively refined using a soft label update mechanism
 117 in conjunction with an enhanced inter-class difference loss
 118 function. This enables the model to dynamically correct and
 119 learn from emotionally ambiguous data. Unlike existing SER
 120 methods that rely on static soft labels, sample reweighting,
 121 or offline label preprocessing, our model performs real-time,
 122 model-driven correction of ambiguous label distributions and
 123 jointly optimizes label refinement and representation learning
 124 within a single end-to-end framework. Moreover, we provide
 125 a theoretical analysis showing that this dynamic correction
 126 process guides the model toward the underlying true emo-
 127 tional distribution despite noisy or subjective annotations.
 128 Experimental results demonstrate that our method outperforms
 129 existing state-of-the-art approaches, particularly in its ability
 130 to effectively handle the ambiguity and subjectivity inherent in
 131 real-world speech emotion recognition. In summary, we make
 132 the following contributions in this paper:

133 1) We propose a novel speech emotion recognition (SER)
 134 approach, designed specifically to handle ambiguous
 135 speech, that addresses some of the key limitations of
 136 existing SER models, including the over-reliance on
 137 subjectively annotated labels, neglect of emotional distri-

138 butions, and the underutilization of ambiguous samples
 139 lacking explicit (hard, consensus) emotion labels.

140 2) We introduce a real-time soft label correction strategy,
 141 theoretically validated to guide the model toward learning
 142 the true emotional distribution, even in the presence of
 143 label noise. This strategy offers a generalizable solution
 144 for other tasks involving noisy/ambiguous annotations.

145 3) We construct a comprehensive spatial-temporal feature
 146 extraction pipeline by combining the representational
 147 strengths of CNNs and Wav2Vec 2.0. Through a novel
 148 multi-level fusion mechanisms, our model effectively in-
 149 tegrates time-frequency emotional cues for robust speech
 150 emotion recognition.

151 It should be noted that in this work, the term spatial speci-
 152 fically refers to the frequency dimension of the spectrogram,
 153 which can be treated analogously to the spatial axis in image
 154 processing when applying 2D-CNNs. The term temporal corre-
 155 sponds to the time dimension, capturing the dynamic evolution
 156 of speech signals.

II. RELATED WORK

157 In this section, we now discuss relevant prior work related to
 158 the research presented in this paper. For a more comprehensive
 159 coverage of the area of speech emotion recognition (SER), the
 160 reader is referred to some of the excellent surveys available in
 161 the literature on this topic, i.e., [6], [20]–[23].

162 Early work in speech emotion recognition (SER) primarily
 163 relied on single-label annotations derived through majority
 164 voting (i.e., **consensus labels** hereafter) across annotators. To
 165 better exploit the spatio-temporal characteristics of speech sig-
 166 nals, Ye *et al.* [24] introduced a time-aware bidirectional scal-
 167 ing network designed to integrate information from both past
 168 and future contexts, thereby enhancing the model’s contextual
 169 representation capabilities. Li *et al.* [25] proposed a model that
 170 combines a spatiotemporal attention mechanism with a large-
 171 horizon learning strategy built on a CNN backbone, effectively
 172 localizing emotional regions while mitigating feature overlap.
 173 Building on this idea, Wu *et al.* [26] replaced attention mod-
 174 ules with a capsule network to improve recognition accuracy
 175 by capturing hierarchical relationships among features. Gan *et*
 176 *al.* [27] developed a spatial-temporal network that integrates
 177 features through multiple fusion strategies, achieving strong
 178 performance in capturing both spatial and temporal cues.

179 While the studies outlined above have significantly ad-
 180 vanced SER through various modeling strategies in the spatial,
 181 temporal, and joint domains, they generally do not address
 182 the issue of ambiguous emotional expressions in speech. To
 183 indirectly tackle this problem, Wang *et al.* [28] leveraged
 184 large language models (LLMs) to generate emotionally rich
 185 synthetic speech data based on a student speech dataset,
 186 while Yu *et al.* [29] applied an Attention-LSTM-Attention
 187 architecture to augmented datasets, aiming to enhance label
 188 robustness and alleviate ambiguity-related challenges. Several
 189 studies have also looked at the model architecture to reduce
 190 the impact of speech ambiguity on emotion recognition. Fan
 191 *et al.* [8], for example, introduced an Individual Standardized
 192 Network (ISNet) that addresses inter-individual variability in

194 emotional expression and, thus, aims to reduce confusion
 195 caused by personalized affective patterns. Yin *et al.* [30]
 196 proposed a progressive co-teaching strategy inspired by human
 197 and animal learning processes, where the model is trained on
 198 samples of increasing complexity (from simple to ambiguous)
 199 to mitigate the negative influence of emotionally ambiguous
 200 data on training stability. While these approaches acknowledge
 201 the challenges posed by emotional ambiguity, they still mostly
 202 rely on single-label annotations and, in turn, fail to capture
 203 the nuanced, multi-dimensional nature of emotional expression
 204 in speech. As a result, these methods suffer from inadequate
 205 feature representation, limiting their ability to fully model the
 206 complexity of real-world emotional speech.

207 Recognizing the limitations of single-label approaches, sev-
 208 eral studies have proposed alternative labeling strategies to
 209 better capture the inherent ambiguity in emotional speech.
 210 These efforts aim to model the coexistence of multiple emo-
 211 tions within a single utterance and account for inter-annotator
 212 variability in emotion perception. Li *et al.* [14], for instance,
 213 employed multiple labels as the ground truth for model
 214 training and introduced an inter-class difference loss function
 215 to reduce the similarity between emotion classes, thereby
 216 facilitating more accurate modeling of emotion distributions.

217 However, while such multi-label approaches can indicate the
 218 presence or absence of emotions, they often fail to distinguish
 219 between dominant and subordinate emotions in speech sam-
 220 ples, which is critical when dealing with ambiguous speech.
 221 The seminal work of Steidl *et al.* [15] introduced soft labels,
 222 which reflect the proportion of annotator votes across emotion
 223 categories to capture perceptual ambiguity more precisely and
 224 addressed this problem. The authors also showed that the
 225 entropy of these soft labels closely aligns with the entropy
 226 of labels generated by an artificial/simulated annotator, sug-
 227 gesting that such soft labels effectively capture the annotators'
 228 perception of ambiguous emotions. Despite this advancement,
 229 most studies employing soft labels rely directly on observed
 230 annotator distributions, failing to account for the underlying
 231 subjectivity and variability in human emotion perception. As
 232 a result, these approaches risk embedding annotator bias into
 233 the training process, which may distort the model's ability to
 234 learn the true emotional content. To address this issue, Fayek
 235 *et al.* [11] proposed modeling individual annotators separately
 236 and integrating their outputs to generate more robust multi-
 237 label representations. Building on this line of work, Ando
 238 *et al.* [31] successfully incorporated speech samples lacking
 239 a single (discrete, consensus) label by modifying the soft-
 240 label representation to accommodate ambiguous expressions.
 241 Subsequently, Ando *et al.* [13] extended this framework by
 242 leveraging soft labels over multi-label annotations in repeated
 243 training runs, enabling a more comprehensive use of the full
 244 dataset, including emotionally ambiguous samples. Neverthe-
 245 less, even these methods fall short of fully addressing annotator
 246 subjectivity, where individual perceptions may diverge
 247 significantly from the consensus, thus, introducing label noise
 248 that can mislead the model and compromise its ability to learn
 249 accurate emotional distributions.

250 In response to the challenges posed by label noise, Wang
 251 *et al.* [32] proposed a unified two-stage framework, con-

sisting of labels noise modeling and correction training, to
 252 address different types of label noise in image classification
 253 tasks. Building on this concept, Liu *et al.* [33] introduced a
 254 validation-based mechanism to determine whether labels in
 255 the training set should be revised and demonstrated improved
 256 model robustness through selective label correction. Inspired
 257 by these label correction strategies, Fujioka *et al.* [34] applied
 258 a meta-learning approach that combines corrected labels with
 259 sample weight estimation to update noisy annotations.
 260

261 In the context of speech emotion recognition, Mao *et al.*
 262 [35] observed that static soft labels fail to capture the dynamic
 263 nature of emotional expression, and, thus, proposed an emotion
 264 profile refinement strategy that generates soft labels in
 265 real time to better represent emotional evolution in speech.
 266 While these approaches mark significant progress in SER,
 267 they still largely neglect samples without consensus labels,
 268 i.e., samples that are most representative of the ambiguity
 269 and uncertainty inherent in natural emotional speech. Ignoring
 270 such training samples limits the ability of classification models
 271 to learn comprehensive and robust emotional representations.
 272 Beyond these general label correction strategies, recent works
 273 have introduced meta-learning and co-teaching frameworks
 274 directly into speech emotion recognition (SER). For example,
 275 Yin *et al.* [36] proposed a progressive co-teaching approach
 276 to mitigate the impact of emotionally ambiguous labels by
 277 iteratively exchanging reliable samples between peer networks.
 278 Chopra *et al.* [37] and Cai *et al.* [38] further explored
 279 meta-learning paradigms for low-resource or multi-task SER,
 280 showing that adaptive reweighting of uncertain annotations
 281 can improve robustness. However, these approaches mainly
 282 rely on sample reweighting or selection, while leaving the
 283 underlying label distributions unchanged, which may limit
 284 their effectiveness for inherently ambiguous emotional speech.
 285

286 Inspired by the research discussed above, we propose in this
 287 paper a novel model for ambiguous speech emotion recogni-
 288 tion. At the core of our approach is an innovative real-time
 289 soft label correction strategy, specifically designed to handle
 290 emotionally ambiguous speech samples. We theoretically and
 291 empirically demonstrate that this strategy effectively captures
 292 the underlying emotional distribution, even in the presence of
 293 noisy or unreliable labels. Furthermore, we leverage the rep-
 294 resentational power of convolutional neural networks (CNNs)
 295 alongside the contextual learning capabilities of Wav2Vec 2.0
 296 to perform a detailed analysis of the speech signal's spa-
 297 tiotemporal characteristics. By employing multi-level feature
 298 fusion, our model efficiently integrates these representations,
 299 and allows for a robust and comprehensive understanding of
 300 speech emotions.

III. SOFT-LABEL CORRECTION STRATEGY

301 A key component of the speech emotion recognition model
 302 proposed in this work is a **novel soft-label correction stra-
 303 tegy**, designed specifically to account for the ambiguity of em-
 304 otional speech and emotion perception from the annotators. In
 305 this section, we first motivate the need for soft-label correction
 306 and then theoretically show that soft-label correction leads to
 307 better ground truth and, in turn, better recognition models.

308 **A. Problem Description**

309 The variability in individual emotion perception typically
 310 leads annotators to assign different emotional labels to the
 311 same speech sample, resulting in samples that are annotated
 312 with multiple labels. In most existing speech emotion recog-
 313 nition (SER) methods, the prevailing approach is to adopt the
 314 emotion category with the highest number of votes as the
 315 final (consensus) label for the utterance. However, this practice
 316 introduces two key limitations:

- 317 1) Human speech frequently conveys a mixture of emotions,
 318 and majority-vote labeling fails to capture the nuanced
 319 and overlapping emotions inherent in natural speech.
- 320 2) Due to the subjectivity of human emotion perception,
 321 annotators often struggle to reach consensus, leading to
 322 uncertainty and ambiguity in soft-label distributions.

323 We propose a real-time soft label correction strategy that
 324 leverages the emotional features extracted through spatiotem-
 325 poral neural networks. This strategy is designed to more
 326 accurately model the subtle emotional variations in speech
 327 while reducing the impact of noisy or ambiguous labels that
 328 could negatively affect model performance. Additionally, we
 329 provide a theoretical foundation to support the effectiveness of
 330 the proposed correction mechanism in learning more reliable
 331 emotional representations.

332 **B. Real-time Soft-Label Correction Strategy**

333 The proposed real-time soft label correction strategy con-
 334 sists of two key components. First, it employs a **dynamic**
 335 **soft label update mechanism** to iteratively refine the soft
 336 labels associated with ambiguous speech segments. This ap-
 337 proach reduces overreliance on potentially noisy ground truth
 338 annotations and enables more accurate emotion representation.
 339 Second, the strategy incorporates a **joint loss function specif-
 340 ically designed to support real-time label refinement**. This
 341 loss function combines a standard cross-entropy term to ensure
 342 stable model training with an enhanced inter-class difference
 343 loss, which encourages greater discrimination between emotion
 344 categories. These components jointly improve the quality
 345 of soft labels and enhance overall model performance.

346 **Soft-Label Updating Mechanism.** The soft label updating
 347 process for ambiguous speech samples is formulated as a
 348 weighted combination of the observed (annotator-provided)
 349 labels and the model-generated predictions. This design is
 350 based on two key observations: (i) deep learning models excel
 351 at capturing complex patterns in data and can produce reliable
 352 emotion predictions from the provided speech samples when
 353 trained effectively, and (ii) the observed annotator provided
 354 labels, though potentially noisy, are generally close approx-
 355 imations of the true emotional states. Thus, combining both
 356 sources through a weighted summation enables the model to
 357 benefit from the provided (prior, potentially noisy) annotations
 358 while gradually incorporating its own learned representations
 359 and thereby improving label quality over time.

360 Importantly, the soft label refinement process is applied
 361 exclusively to ambiguous speech samples. For unambiguous
 362 samples, annotated with a consensus label, the original labels

363 are retained without modification. This is based on the premise
 364 that clearly expressed emotions are less prone to annotator
 365 disagreement and are thus less likely to contain labeling errors.
 366 From this perspective, we classify all speech samples in a
 367 given dataset into two disjoint subsets:

- 368 • **Clear samples** (S_A), i.e., samples with (single) discrete
 369 consensus labels that exhibit strong agreement across
 370 annotators w.r.t. the expressed emotion.
- 371 • **Ambiguous samples** (S_B), i.e., samples associated with
 372 multiple labels that reflect disagreement among annota-
 373 tors and emotional uncertainty.

374 Let S denote the full set of speech samples, such that
 375 $S = S_A \cup S_B$ and $S_A \cap S_B = \emptyset$. Furthermore, let N_1 , N_2 ,
 376 and N be the number of clear samples in S_A , ambiguous
 377 samples in S_B , and samples in the complete set S , respectively.
 378 In a supervised K -class classification task, the labels corre-
 379 sponding to the set of clear samples S_A are single (consensus)
 380 labels $y_{cons}^{x^i}$, defined as the emotion categories considered by
 381 the majority of annotators, i.e.:

$$y_{cons}^{x^i} = (y_1^{x^i}, y_2^{x^i}, \dots, y_K^{x^i}), y_j^{x^i} \in \{0, 1\}, \quad (1)$$

382 where $\sum y_j^{x^i} = 1, i \in \{1, \dots, N_1\}$, $x^i \in S_A$ denotes
 383 the i^{th} speech sample. A value of $y_j^{x^i} = 1$ indicates that
 384 the majority of annotators assigned the j^{th} emotion class to
 385 sample x^i , whereas a value of 0 indicates otherwise. This one-
 386 hot encoding reflects the assumption that each clear sample is
 387 associated with a single dominant emotion.

388 However, due to the limited number of annotators and
 389 the inherently subjective nature of emotion perception, many
 390 samples exhibit label ambiguity. These ambiguous samples (in
 391 S_B) are characterized by inconsistent annotator opinions and
 392 are labeled using multi-label representations $y_{multi}^{x^i}$, i.e.:

$$y_{multi}^{x^i} = (t_1^{x^i}, t_2^{x^i}, \dots, t_K^{x^i}), t_j^{x^i} \in \{0, Z_+\}, x^i \in S_B, \quad (2)$$

393 where, $i \in \{1, \dots, N_2\}$, Z_+ denotes the set of positive
 394 integers, and N_2 is the number of ambiguous samples in S_B .
 395 Here $t_j^{x^i}$ represents the number of annotators who assigned
 396 the j^{th} emotion label to speech sample x^i , capturing the
 397 distribution of annotator responses. Since this form is not
 398 directly compatible with standard model training objectives,
 399 it is often converted to a binary multi-label form, as in [14]:

$$y_{multi}^{x^i} = (s_1^{x^i}, s_2^{x^i}, \dots, s_K^{x^i}), s_j^{x^i} \in \{0, 1\}, x^i \in S_B, \quad (3)$$

400 where $i \in \{1, \dots, N_2\}$, and $s_j^{x^i} = 1$ (or 0) indicates whether
 401 at least one annotator perceived (or did not perceive) the
 402 presence of the j^{th} emotion in sample x^i . It is evident that
 403 Eq. (1) is a special case of Eq. (3), i.e., when $\sum s_j^{x^i} = 1$, both
 404 formulations are equivalent.

405 Nevertheless, this multi-label representation does not reflect
 406 the relative prevalence of each emotion in the given speech
 407 sample. To address this limitation, soft-labels $y_s^{x^i}$, which
 408 capture the proportion of annotator votes for each emotion
 409 class, are commonly used instead. Here, soft-labels are defined
 410 as a probability distribution over the K emotion classes: i.e.:

$$y_s^{x^i} = (p_1^{x^i}, p_2^{x^i}, \dots, p_K^{x^i}), p_j^{x^i} \in [0, 1], \quad (4)$$

411 where $\sum p_j^{x^i} = 1$, $i \in \{1, \dots, N_2\}$, and each $p_j^{x^i}$ is computed
412 as:

$$p_j^{x^i} = \frac{t_j^{x^i}}{\sum_m^K t_m^{x^i}}, \quad (5)$$

413 with $t_j^{x^i}$ denoting the number of annotators who assigned the
414 j^{th} emotion label to sample x^i . This formulation captures
415 the proportion of votes per class and reflects the perceived
416 emotional distribution. However, due to the limited number of
417 annotators and the subjectivity of emotion perception, these
418 soft labels may still contain inaccuracies and may not fully
419 reflect the true emotional composition of the speech sample.
420 To alleviate this problem, we introduce a *soft-label update*
421 *mechanism* that generates corrected soft-labels $y_c^{x^i}$ as follows:

$$y_c^{x^i} = \begin{cases} y_{cons}^{x^i}, & x^i \in S_A, \\ (1 - \alpha)y_s^{x^i} + \alpha y_g^{x^i}, & \alpha \in [0, 1], x^i \in S_B, \end{cases} \quad (6)$$

422 where $y_c^{x^i}$ denotes the corrected labels for sample x^i , $y_s^{x^i}$
423 stands for the original soft label and $y_g^{x^i}$ is the label predicted
424 by the emotion recognition model for the same sample. The
425 parameter $\alpha \in [0, 1]$ is a correction coefficient that controls
426 the contribution of the model-generated prediction to the final
427 soft label. For clear samples ($x^i \in S_A$) the original consensus
428 label is retained, while for ambiguous samples ($x^i \in S_B$), the
429 corrected label is obtained through a weighted combination of
430 the original soft label and the model-generated label.

431 **The Joint Loss Function.** The overall training objective
432 for our model is defined by a joint loss function L , which
433 combines two components: a cross-entropy loss L_{cor} for
434 optimizing model predictions, and an enhanced inter-class
435 difference loss L_{Ic} designed for real-time soft-label correction.

436 The cross-entropy loss L_{cor} quantifies the divergence be-
437 tween the predicted emotion distributions and the target labels
438 and is widely used in supervised classification tasks. It is
439 formulated as:

$$L_{cor} = -\frac{1}{N} \sum_{i=1}^N \sum_{j=1}^K y_j^{x^i} \log(p_j^{x^i}), \quad x^i \in S, \quad (7)$$

440 where the predicted probability $p_j^{x^i}$ for class j is
441 computed via the softmax function:

$$p_j^{x^i} = \frac{\exp(o_j^{x^i})}{\sum_{k=1}^K \exp(o_k^{x^i})}. \quad (8)$$

442 Here, N denotes the total number of training samples, $o_j^{x^i}$
443 is the model output (logit) for class j , $y_j^{x^i} \in [0, 1]$ is the
444 target label (either consensus or soft label) and $p_j^{x^i}$ denotes the
445 predicted probability for emotion class j in speech sample x^i .

446 To support the dynamic correction of soft labels for am-
447 biguous samples, an additional loss term L_{Ic} is introduced.
448 This enhanced inter-class difference loss acts as a regular-
449 ization mechanism, guiding the model-generated labels $y_g^{x^i}$
450 to remain consistent with the observed soft labels $y_s^{x^i}$, while
451 mitigating overfitting, particularly when the dataset contains a
452 large proportion of ambiguous samples. Unlike the inter-class

453 difference loss originally proposed in [14], which assumes
454 binary labels, the enhanced version here accommodates soft
455 labels $y_j^{x^i} \in \{0, 1\}$. The loss is defined as:

$$L_{Ic} = \begin{cases} 0, & x^i \in S_A, \\ \frac{1}{N_2} \sum_{i=1}^N \sum_{j=1}^K \sum_{k=1}^K (\exp(u) - 1), & x^i \in S_B, \end{cases} \quad (9)$$

456 where

$$u = \max \left\{ 0, \left(1 - y_j^{x^i} \right) (p_j^{x^i} + \beta) - y_j^{x^i} p_k^{x^i} \right\}. \quad (10)$$

457 Here, $x^i \in S_B$ denotes an ambiguous speech sample, $y_j^{x^i} \in$
458 $[0, 1]$ is the corrected soft label for class j , $p_j^{x^i}$ is the
459 corresponding predicted probability, and β is a margin control
460 coefficient that regulates the separation between class predi-
461 cations. This loss encourages higher inter-class discrimination,
462 especially in ambiguous contexts. Given the bounded nature of
463 $y_j^{x^i}$, β , and $p_k^{x^i}$, the value of L_{Ic} is constrained to the interval
464 $[0, k^2(\exp(2) - 1))$.

465 The final joint loss L used for training is the sum of the
466 two components, i.e.:

$$L = L_{cor} + L_{Ic}. \quad (11)$$

C. Feasibility Analysis

467 In the previous section, we introduced the real-time soft
468 label correction strategy. In this section we now present a theo-
469 retical analysis and a formal proof to validate the effectiveness
470 of the proposed strategy.

471 **Proof Overview.** The main idea of the proof is to demonstrate
472 that, under a reasonable setting of the correction coefficient α
473 and margin control coefficients β , the model parameters θ'_M
474 obtained through the real-time soft label correction strategy
475 can converge to a region near the optimal parameters θ_t , which
476 are obtained using the true label distribution. In other words,
477 the strategy effectively guides the training process toward the
478 underlying ground-truth distribution despite the presence of
479 noisy or ambiguous labels. To support this claim, we first
480 present two foundational lemmas:

481 **Lemma 1.** *There exists a two-layer neural network with*
482 *ReLU (Rectified Linear Unit) activation functions and $2n + d$*
483 *parameters that can represent any function over a dataset of*
484 *n samples in a d -dimensional space [39].*

485 Lemma 1 implies that a sufficiently parameterized deep neural
486 network can approximate any label distribution, regardless of
487 the choice of loss function.

488 **Lemma 2.** *Assuming a neural network with sufficient capacity,*
489 *for any loss function, L , the training dynamics follow the*
490 *convergence path: $f_{\theta_0} \rightarrow f_{\theta_t} \rightarrow f_{\theta_*}$, where f_{θ_0} is the*
491 *is the model initialized with random parameters θ_0 , f_{θ_t} is*
492 *is the model trained with true (clean) labels, and, and f_{θ_*}*
493 *corresponds to the model trained with observed (possibly*
494 *noisy) labels [33].*

496 Lemma 2 suggests that while training may begin with ran-
 497 dom initialization, convergence paths under true labels and
 498 observed labels are both attainable and related.

499 Building upon these lemmas, the following theorem pro-
 500 vides the basis for analyzing the behavior of the proposed
 501 correction strategy:

502 **Theorem 1.** *Let θ_t denote the model parameters after t
 503 optimization steps using true labels, and let θ_M denote the
 504 parameters after M steps ($M > t$) using observed, poten-
 505 tially noisy labels. Then, the final parameters θ_M lie with a
 506 neighborhood of θ_t , i.e., $\theta_M \in [\theta_t - R_M, \theta_t + R_M]$, where
 507 R_M denotes the radius of the neighborhood that quantifies
 508 the deviation caused by label noise.*

509 Theorem 1 implies that if the label correction mechanism
 510 effectively reduces the noise in observed labels (by leveraging
 511 model-generated predictions and controlling the correction
 512 dynamics via α and β) then the model can be guided to
 513 converge toward a representation close to that obtained under
 514 true labels.

515 *Proof:* According to Lemma 1, a sufficiently parameterized
 516 model can fit any label distribution and will converge after at
 517 most M optimization steps. Lemma 2 further states that the
 518 model, initialized at θ_0 reaches the parameter state θ_t after t
 519 iterations when trained on true ground truth labels y_{true} . Let us
 520 consider the standard parameter update rule in deep learning.
 521 At iteration $t+1$ the model parameters are updated as follows:

$$\theta_{t+1} = \theta_t - lr \cdot g(\theta) \Big|_{\theta=\theta_t}, \quad (12)$$

522 where lr is the learning rate, and $g(\theta) = \frac{\partial L}{\partial \theta}$ denotes the
 523 gradient of the loss function L with respect to the parameters.
 524 By recursively applying this update rule, the model parameters
 525 at iteration M can be expressed as:

$$\theta_M = \theta_t - lr \sum_{i=0}^{M-t-1} g(\theta) \Big|_{\theta=\theta_{t+i}}. \quad (13)$$

526 Let us define the average gradient during the convergence
 527 process as: $\psi = \frac{1}{M-t} \sum_{i=0}^{M-t} \frac{\partial L}{\partial \theta_{t+i}}$. Since this expression is
 528 bounded for all $t+i \in [t, M-1]$, the average gradient ψ
 529 satisfies:

$$\min_{t \leq i \leq M-1} \{g(\theta)\Big|_{\theta_i}\} \leq \psi \leq \max_{t \leq i \leq M-1} \{g(\theta)\Big|_{\theta_i}\}. \quad (14)$$

530 From Eq. (14), it follows that the final model parameters
 531 θ_M lie within a neighborhood around the true label-trained
 532 parameters θ_t with a radius defined by the learning rate and
 533 maximum gradient norm:

$$\theta_M \in \{\theta | \theta_t - R_M \leq \theta \leq \theta_t + R_M\}, \quad (15)$$

534 where $R_M = lr \max\{|g(\theta_t)|, \dots, |g(\theta_{M-1})|\}$.

535 According to Theorem 1, when the real-time soft label
 536 correction strategy is applied, the gradient $g(\theta)$ is defined as:

$$g(\theta) = \begin{cases} \sum_{i=1}^N \sum_{j=1}^K \left(\frac{m}{N^2} \sum_{k=1}^K v_{ijk} \exp(u_{ijk}) - \frac{(y_c)_j^{x^i}}{N p_j^{x^i}} \right), \\ m = 0, x^i \in S_A, \\ m = 1, x^i \in S_B, \\ (y_c)_j^{x^i} = (y_{cons})_j^{x^i}, x^i \in S_A, \\ (y_c)_j^{x^i} = (1 - \alpha)(y_s)_j^{x^i} + \alpha p_j^{x^i}, x^i \in S_B, \\ u_{ijk} = (1 - (y_s)_j^{x^i})(p_j^{x^i} + \beta) - (y_s)_j^{x^i} p_k^{x^i}, \\ v_{ijk} = (1 - (y_s)_j^{x^i}) - (y_s)_k^{x^i} \frac{\partial p_k^{x^i}}{\partial p_j^{x^i}}. \end{cases} \quad (16)$$

537 Eq. (16) indicates that the gradient and, hence, the convergence
 538 behavior of the model is directly influenced by the correction
 539 coefficient α and the margin control coefficient β . These
 540 parameters modulate the extent to which model predictions
 541 correct or align with the soft labels, thereby controlling the
 542 size of the radius R_M in which convergence occurs.

543 **Theorem 2.** *Let $M (x^i | \theta)$ be a training network converging
 544 at iteration M iteration using observation labels and yielding
 545 model parameters θ_M . Suppose the observation labels are
 546 subsequently corrected and the network is retrained. Upon
 547 convergence after M iterations with corrected labels, the
 548 resulting parameters θ'_M lie within a neighborhood of θ_M ,
 549 i.e., $\theta'_M \in [\theta_M - R'_M, \theta_M + R'_M]$, where R'_M is the radius of
 550 the neighborhood.*

551 *Proof:* According to Theorem 1, the parameters θ_M , ob-
 552 tained after training with observation labels, lies within a
 553 neighborhood of the true-label parameters θ_t , such that

$$\begin{cases} \theta_M = \theta_t + n_1 R_M, n_1 \in [-1, 1], \\ \theta'_M = \theta_t + n_2 R'_M, n_2 \in [-1, 1]. \end{cases} \quad (17)$$

554 where R_M and R'_M are the neighborhood radii associated with
 555 training under observation labels and corrected labels, respec-
 556 tively. n_1 and n_2 are scaling constants reflecting directional
 557 distance. It follows that θ'_M can be expressed relative to θ_M
 558 as:

$$\theta'_M = \theta_M + n R'_M = \theta_M + n_2 R'_M - n_1 R_M, n \in [-1, 1]. \quad (18)$$

559 Thus, $\theta'_M \in [\theta_M - R'_M, \theta_M + R'_M]$, confirming that the
 560 corrected-label solution lies in the vicinity of the original
 561 observation-label solution, where n is a constant and R'_M is
 562 the neighborhood radius.

563 Fig. 1 illustrates two possible relationships between the
 564 neighborhoods defined by Theorems 1 and 2. Here:

- 565 • O_1 represents the region around θ_M with radius R'_M ,
 566 within which θ'_M is located.
- 567 • O_2 represents the region centered at θ_t , defined by the
 568 original radius R_M .

569 In both scenarios, the shaded area denotes regions where
 570 θ'_M is closer to θ_t than θ_M . Since observation labels are fixed
 571 for a given dataset, the size of neighborhood O_2 remains
 572 approximately constant for a given model. Let's define the
 573 proportion of the shaded area S to the area of O_1 , denoted as
 574 S_{O_1} , as:

$$P = \frac{S}{S_{O_1}}. \quad (19)$$

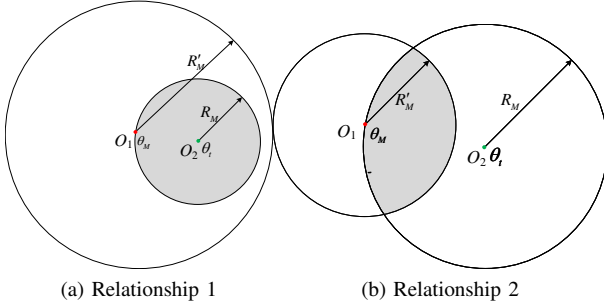


Fig. 1: **Illustration of the relationship** between the two neighborhoods identified in Theorem 1 and Theorem 2

575 A higher value of P indicates a greater probability that θ'_M lies closer to the true-label parameters θ_t than θ_M . For a 576 constant R_M , the probability P increases as R_M decreases. 577 The correction radius R'_M is influenced by the correction 578 coefficient α and the margin control coefficients β . This 579 control relationship can be expressed as:

$$(\alpha, \beta) \rightarrow (R_M, R'_M) \rightarrow R'_M \rightarrow P \quad (20)$$

581 where \rightarrow denotes the directional influence of the preceding 582 variables on the subsequent ones.

583 In summary, by appropriately tuning α and β , it is possible 584 to reduce the neighborhood radius R'_M , thereby guiding θ'_M 585 closer to θ_t than θ_M , which establishes the theoretical 586 feasibility and effectiveness of the proposed real-time soft label 587 correction strategy.

IV. THE PROPOSED METHOD

589 In this section, we now present the main contribution of this 590 work, i.e., our **novel model for speech emotion recognition**, 591 designed specifically to handle ambiguous speech samples. 592 We start the section with a brief high-level description of the 593 proposed approach and then proceed with the description of 594 the individual components.

595 A. Overview

596 Speech emotion recognition remains challenging due to 597 label ambiguity, subjective annotation noise, and the complex 598 temporal-spectral dynamics of speech signals, as discussed 599 in the Introduction. To address these challenges, we propose 600 an enhanced ambiguous speech emotion recognition model, 601 illustrated in Figure 2. The model architecture consists of five 602 main components that are described in detail in the following 603 sections, i.e.: (i) a spatial feature extraction module (§IV-B), 604 a temporal module (§IV-C), a multi-level fusion module 605 (§IV-D), a real-time soft label correction module (§IV-E), and 606 a classification module that determine the final emotion class 607 of the input speech sample (§IV-F).

608 B. The Spatial Module

609 We use Log Mel-Filter Bank (Fbank) features as the input, 610 which form a conventional time-frequency spectrogram

widely adopted in speech and audio processing. This representation provides a two-dimensional structure suitable for CNN-based modeling. The resulting Fbank feature maps are fed into a convolutional network, i.e., the spatial domain module, for hierarchical emotion feature extraction. The architecture of this module is illustrated in Figure 3.

To align with the input format expected by 2D convolutional layers, we first reshape the extracted Fbank features into a three-dimensional tensor $X_{in} \in \mathbb{R}^{1 \times f \times M}$, where '1' denotes the input channel dimension required by 2D-CNNs, f denotes the number of frames and M represents the number of Mel filter banks. This representation preserves the two-dimensional time-frequency structure of speech, which is essential for learning emotion-relevant spatial patterns.

Given that each Fbank feature map captures spectral information over a sequence of frames, we design a **parallel convolutional structure** to extract features along different axes of the time-frequency domain. Specifically, we apply three parallel convolutional operations: one emphasizing temporal patterns, another focusing on spectral characteristics, and a third capturing joint time-frequency dependencies. Unlike conventional CNN-based SER approaches that apply uniform 2D kernels directly on spectrograms, our parallel design explicitly separates temporal, spectral, and joint Spatio-temporal modeling through distinct kernel shapes (11×1, 1×9, and 5×5). This decomposition enables the model to capture complementary emotional cues from different perspectives before fusing them into a unified representation. The output of this parallel convolution block is defined as:

$$X_c = C(Conv^{1a}(X_{in}), Conv^{1b}(X_{in}), Conv^{1c}(X_{in})), \quad (21)$$

where $X_c \in \mathbb{R}^{24 \times \frac{f}{2} \times \frac{M}{2}}$, and $C(\cdot)$ denotes channel-wise concatenation. The operations $Conv^{1a}(\cdot)$, $Conv^{1b}(\cdot)$, and $Conv^{1c}(\cdot)$ correspond to convolution layers designed to capture temporal, spectral, and joint temporal-spectral features, respectively.

To further deepen the representation and aggregate mid-level features, we pass X_c through five consecutive convolutional layers using 3×3 kernels. These layers progressively refine the feature maps while reducing spatial resolution. Notably, no downsampling is applied after the final convolution to preserve critical information. The resulting feature map X_d is given by:

$$X_d = Conv^5(X_c), \quad X_d \in \mathbb{R}^{96 \times \frac{f}{32} \times \frac{M}{32}}, \quad (22)$$

where $Conv^5(\cdot)$ represents the stacked five-layer convolutional block. Finally, we apply global average pooling (GAP) to compress the spatial feature map into a fixed-dimensional embedding $X_s \in \mathbb{R}^{96}$, which serves as the output of the spatial domain module:

$$X_s = GP(X_d), \quad X_s \in \mathbb{R}^{96}, \quad (23)$$

where $GP(\cdot)$ denotes global average pooling. This operation summarizes the learned spatial features into a compact representation suitable for downstream fusion and classification.

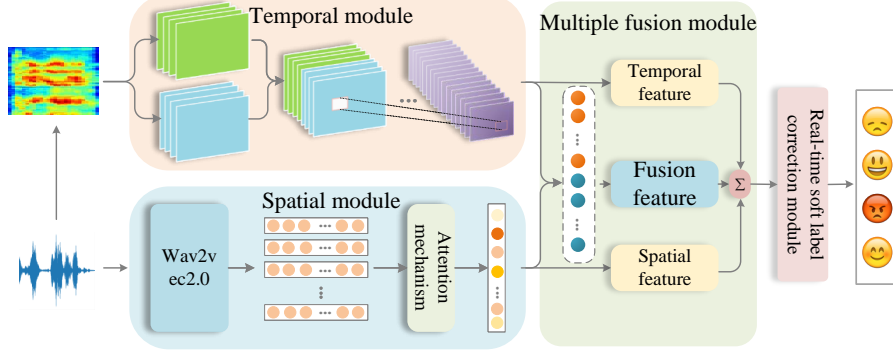


Fig. 2: **High-level overview** of the proposed ambiguous speech emotion recognition model. The model integrates a spatio-temporal feature extraction module based on dedicated CNN and Wav2Vec 2.0, followed by multi-level fusion to capture complementary emotional cues. A real-time soft label correction module is also designed to dynamically refine ambiguous labels during training using a combination of cross-entropy and enhanced inter-class difference losses.

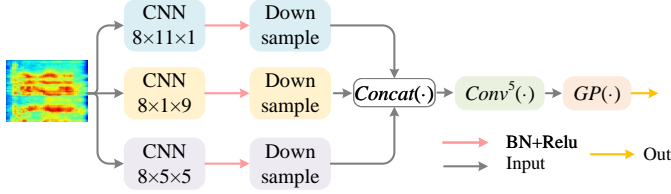


Fig. 3: **Structure of the spatial module.** The module operates on a time-frequency representation of the input speech. It employs three parallel convolutional branches with kernel sizes of 11×1 , 1×9 , and 5×5 , respectively, corresponding to temporal, spectral, and joint Spatio-temporal modeling. Each branch outputs 8 feature maps, where “8” denotes the number of convolutional filters (channels) used to capture diverse patterns.

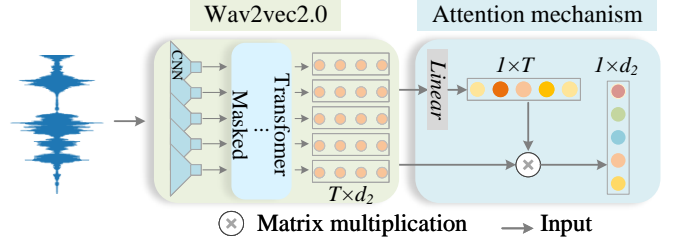


Fig. 4: **Structure of temporal module.** We use Wav2Vec 2.0 to extract high-level temporal features from raw speech waveforms using convolution, masking, and transformer blocks.

eling objectives during fine-tuning, a masking operation is applied to G' , yielding:

$$F_1 = \text{Mask}(G') \in \mathbb{R}^{T \times d_2}, \quad (25)$$

where $\text{Mask}(\cdot)$ randomly masks segments of the sequence. The masked features are then passed through the Transformer encoder of Wav2Vec 2.0:

$$F_2 = \text{Transformer}(F_1) \in \mathbb{R}^{T \times d_2}. \quad (26)$$

To obtain a fixed-length temporal feature vector, we apply another linear transformation followed by a weighted aggregation using matrix multiplication:

$$F'_2 = \text{Linear}(F_2), \quad F'_2 \in \mathbb{R}^{1 \times T}, \quad (27)$$

$$F_t = F'_2 \otimes F_2, \quad F' \in \mathbb{R}^{1 \times T}, \quad F_t \in \mathbb{R}^{1 \times d_2}, \quad (28)$$

where \otimes denotes matrix multiplication. The resulting vector F_t represents the aggregated temporal features of the input speech that captures high-level emotional information across the entire sequence.

D. The Multi-level Fusion Module

Since analyzing temporal or spatial features in isolation limits the model’s ability to fully capture the multifaceted nature of speech signals, we introduce a **multi-level fusion module** to integrate both temporal and spatial emotion representations. This design allows the model to comprehensively

C. The Temporal Module

Speech waveforms are continuous-time signals, and crucial emotion-related information is often embedded in their temporal variations. Accurately modeling these dynamic is thus essential for robust speech emotion recognition. To this end, we leverage Wav2Vec 2.0, a powerful self-supervised representation learning framework pre-trained on large-scale speech corpora. Its strong contextual encoding capabilities provide valuable a priori knowledge, allowing it to effectively extract rich temporal emotion features from raw waveforms.

The temporal module, illustrated in Figure 4, is employed to extract such features directly from the input waveform.

Given an input temporal speech waveform x_i we first apply a series of one-dimensional convolutional layers to produce a feature map $G \in \mathbb{R}^{T \times d_1}$, where T corresponds to the number of frames (which varies with input length), and d_1 is the feature dimension. A linear transformation is then applied to project G into a new representation space:

$$G' = \text{Linear}(G), \quad G' \in \mathbb{R}^{T \times d_2}, \quad (24)$$

where d_2 denotes the dimension of the transformed features. To improve robustness and simulate masked language mod-

698 learn emotional cues that are distributed across time and
699 frequency dimensions.

700 First, we obtain an intermediate fused representation F_{st}
701 by concatenating the spatial emotion feature $X_s \in \mathbb{R}^{d_1}$ and
702 temporal emotion feature $F_t \in \mathbb{R}^{d_2}$, followed by a series of
703 fully connected layers with ReLU activations:

$$F_{st} = \delta \left(C(X_s, F_t) W_f^1 + B_f^1 \right) W_f^2 + B_f^2 \left(W_f^3 + B_f^3 \right), \quad (29)$$

704 where $C(\cdot)$ denotes the concatenation operation, $\delta(\cdot)$ is the
705 ReLU activation, and W_f^i, B_f^i (for $i = 1, 2, 3$) are trainable
706 weight and bias parameters. This operation maps the concatenated
707 features into a joint representation space that enables
708 interaction between the temporal and spatial modalities.

709 Next, to produce the final fused representation F'_{st} , we
710 perform a soft aggregation by applying a softmax function to
711 the sum of three components: linear projections of the spatial
712 and temporal features, and the intermediate fused vector:

$$F'_{st} = \text{softmax} (Linear_s(X_s) + Linear_t(F_t) + F_{st}), \quad (30)$$

713 where $Linear_s(\cdot)$ and $Linear_t(\cdot)$ are learnable linear trans-
714 formations specific to the spatial and temporal features, re-
715 spectively, and $F'_{st} \in \mathbb{R}^{d_t}$ is the final fusion representation
716 of dimension d_t . The presented multi-level fusion mechanism
717 allows the model to not only learn combined feature represen-
718 tations but also dynamically adjust the contribution of each
719 modality during prediction.

720 E. The Real-time Soft-Label Correction Module

721 In Section III, we described the real-time soft label correc-
722 tion strategy in detail and provided a theoretical justification
723 for its effectiveness. In this section, we now apply the proposed
724 strategy directly within our training framework. The complete
725 process is outlined in Algorithm 1.

Algorithm 1 Real-Time Soft Label Correction Strategy

Input: Speech sample set $S = S_A \cup S_B$, where $S_A \cap S_B = \emptyset$
Output: Real-time corrected label $y_j^{x^i}$

- 1: Fine-tune model $M_1(x^i \mid \theta)$ using clear speech samples S_A to obtain M_{1p}
- 2: Integrate fine-tuned model M_{1p} with randomly initialized model $M_2(x^i \mid \theta)$ to form model M_p
- 3: Randomly shuffle samples and input speech $x^i \in S$ into model M_p
- 4: **for** each sample $i = 1$ to N **do**
- 5: Extract features: $F'_{st} = M_p(x^i)$
- 6: **if** $x^i \in S_B$ **then**
- 7: Update label: $y_c^{x^i} = \Omega(y_s^{x^i}, F'_{st})$, where $\Omega(\cdot)$ is the label update function
- 8: **else**
- 9: Assign original label: $y_c^{x^i} = y_{cons}^{x^i}$
- 10: **end if**
- 11: Compute loss: $Loss = L(F'_{st} \mid M_p, y_c^{x^i})$
- 12: **end for**

726 **Notation clarification:** For clarity, the main notations in
727 Algorithm 1 are summarized as follows: θ denotes the model
728 parameters; N is the total number of training samples; $y_j^{x^i}$
729 represents the soft-label probability of sample x^i for class j ;
730 and H_{st}^i indicates the sequence features extracted from sample
731 x^i .

732 In this algorithm, we begin by fine-tuning the network
733 $M_1(x^i \mid \theta)$ using clear-labeled samples from S_A , resulting
734 in model M_{1p} , which captures reliable emotional tendencies.
735 This step mitigates the potential negative impact of ambiguous
736 speech during training. The complete dataset S is then passed
737 through the composite model M_p . For each input $x^i \in S$, if the
738 sample belongs to the ambiguous set S_B , its label is updated
739 using the real-time soft label correction function $\Omega(\cdot)$. If the
740 sample belongs to the clear set S_A , the original (hard) con-
741 sensus label is retained. Finally, the model prediction and the
742 corrected label are used to compute the loss $L(F'_{st} \mid M_p, y_c^{x^i})$.

743 F. Classification

744 The final classification component of the proposed model
745 employs a multi-layer fully connected neural network. This
746 structure is designed to perform fine-grained learning over
747 the distributed emotional features and effectively map them
748 to discrete emotion categories. The classification process is
749 formulated as follows:

$$\hat{y}(x^i \mid M_p) = \text{softmax}(\hat{y}^{x^i}), \quad (31)$$

750 where $\hat{y}(x^i \mid M_p)$ denotes the predicted probability distri-
751 bution over the emotion classes for the input speech sample
752 x^i , and \hat{y}^{x^i} represents the output of the final fully connected
753 layer based on the features extracted by the model M_p . The
754 use of the softmax function ensures that the output forms a
755 valid probability distribution over all emotion categories and
756 facilitates effective multi-class classification.

757 V. EXPERIMENTS

758 In this section, we conduct a rigorous experimental evalua-
759 tion of the proposed speech emotion recognition model and
760 report results that: (i) compare our approach to competing
761 state-of-the-art methods from the literature, (ii) explore the
762 impact of various model components through an ablation
763 study, (iii) investigate the impact of the hyperparameters α
764 and β on classification performance, (iv) study the impact of
765 the model’s learning objective, and (v) analyze the generated
766 embedding space.

767 A. Experimental Setup

768 The proposed model is implemented using PyTorch, utilizing
769 a 64-bit Ubuntu 22.04 system equipped with an NVIDIA
770 RTX 3090 GPU for training and testing.

771 Table I outlines the parameter settings for the training
772 procedure. Unless otherwise specified, the soft-label correction
773 (SLC) phase adopts the same optimizer and fixed learning rate
774 (1e-5) as the fine-tuning stage. The masking probability fol-
775 lows the default configuration of the HuggingFace Wav2Vec2-
776 base-960h model. The training begins by fine-tuning the
777 Wav2Vec 2.0 model using the set of clear samples S_A ,
778 resulting in an intermediate model M_{1p} . This step initializes
779 the model with a domain-specific emotional representation
780 aligned with the IEMOCAP dataset. Subsequently, M_{1p} is
781 integrated with the null-domain module M_2 to construct the
782 complete soft-label correction model M_p , which is then used to

TABLE I: **Parameter settings** utilized during the training procedure of the proposed speech emotion recognition model.

Name	Value
α	0.3
ε	$1e - 5$
β	0.1
Batch size	16
Optimizer	Adam
Learning rate	$1e - 5$
Weight decay	0.0001
Max epoch	100
Early stopping patience	16

783 learn the underlying emotional distribution across all samples,
784 including ambiguous ones. To address class imbalance caused
785 by differing frequencies of emotion categories, the inverse
786 class frequency is employed as the class-wise weight in the
787 loss function during training. This ensures that minority emotion
788 classes are not underrepresented in the learning process.

789 For evaluation, a Leave-One-Speaker-Out (LOSO) cross-
790 validation strategy is adopted, following standard practice in
791 speech emotion recognition research [14], [18]. In this setup,
792 the speech data from one speaker is reserved as the validation
793 set in each fold, while the remaining data is used for training.

794 To ensure a comprehensive performance evaluation, two
795 commonly used metrics are reported for our experiments:
796 Weighted Accuracy (WA) and Unweighted Accuracy (UA)
797 [40], [41]. WA reflects the overall classification accuracy
798 across all utterances, accounting for class distribution, while
799 UA measures the average accuracy across all emotion classes,
800 treating each class equally regardless of frequency.

801 B. Datasets

802 Given that the primary goal of this study is to address the
803 challenge of label noise and improve the model's ability to
804 learn genuine emotional distributions from potentially noisy
805 annotations, the Interactive Emotional Dyadic Motion Capture
806 (IEMOCAP) dataset [42] is selected for experimentation, as it
807 is (to the best of our knowledge) the only publicly available
808 multi-label dataset suitable for our experiments.

809 The IEMOCAP dataset consists of recordings of five dyadic
810 sessions involving 10 actors (5 male, 5 female) in two types
811 of scenarios: scripted dialogues and spontaneous improvisations.
812 The dataset includes rich multimodal data such as
813 audio, video, and text, captured during interactive emotional
814 exchanges between participants. To investigate both the ambi-
815 guity inherent in emotional expression and the subjectivity of
816 emotional perception, we follow the experimental protocol
817 of [34], which utilizes samples from both improvised and
818 scripted settings. Four commonly studied emotion categories,
819 i.e., anger, happiness, sadness, and neutrality, are selected as
820 the target classes for the evaluation.

821 In this study, we focus on the IEMOCAP dataset because
822 it aligns well with the objectives of our method and provides
823 the necessary conditions for evaluation. It contains multi-label
824 annotations, sufficiently ambiguous emotional samples, and
825 diverse speakers that enable leave-one-speaker-out (LOSO)

TABLE II: **Dataset (IEMOCAP) partitioning** used in the experiments. S_A represents clear and S_B ambiguous samples.

Session	Session 1	Session 2	Session 3	Session 4	Session 5
S_A	1316	1248	1324	1216	1494
S_B	726	801	973	1059	890

validation to examine model generalization. Hence, we adopt
826 IEMOCAP as the benchmark corpus to ensure both exper-
827 imental feasibility and fair comparison with prior work.

829 C. Data preprocessing

830 Inspired by the findings in [43], we observe that speech seg-
831 ments with a duration of 7 seconds typically contain sufficient
832 information for effective emotion recognition. Therefore, we
833 segment utterances longer than 7 seconds into fixed 7-second
834 intervals. For shorter utterances, particularly those less than
835 1.5 seconds in length, which we found to be suboptimal for
836 processing by the Wav2Vec 2.0 model, we apply zero-padding
837 to extend them to at least 1.5 seconds. To ensure that emotional
838 cues are preserved and properly learned by the model, we
839 apply zero-padding at the end of the audio rather than at the
840 beginning or middle. After applying these preprocessing steps,
841 we partition the dataset as detailed in Table II.

842 During the feature extraction stage, we convert all original
843 speech signals to digital form at a 16 kHz sampling rate. We
844 apply pre-emphasis filtering to amplify high-frequency com-
845 ponents, which are often critical for emotion-related spectral
846 features. We then compute logarithmic Mel filter bank (MFB)
847 energy features [44], [45], using 40 Mel filters, a 40 ms
848 Hamming window, and a 10 ms frame shift. These features
849 serve as input to our models for both training and evaluation.

850 D. Comparison Methods

851 To rigorously evaluate the proposed method, we select a
852 range of state-of-the-art models for comparison, all of which
853 explicitly address the challenge of speech ambiguity. The
854 goal of the comparative analysis is to highlight the superior
855 performance and notable advantages of our model in handling
856 ambiguous speech.

857 The baseline models considered in our experiments take
858 different strategies to mitigate the negative impact of emotional
859 ambiguity in speech emotion recognition and can be broadly
860 categorized into three groups: (i) models that enhance dataset
861 reliability [28], [29] or exploiting multiple feature represen-
862 tations [30], (ii) models that directly utilize the observation
863 labels of ambiguous speech without further label refinement
864 [14], [31], and (iii) models that update ambiguous observation
865 labels before training to better model true emotional distri-
866 butions [13], [34].

867 It is worth noting that other studies have explored speech
868 emotion recognition based solely on single-label strategies
869 [27], [46]. These works tend to neglect the intrinsic ambiguity
870 and complexity of emotional expression in speech and are,
871 therefore, not considered in this work. Similarly, models
872 leveraging fusion techniques across different modalities (e.g.,

873 speech and text) [47], [48] attempt to compensate for the
 874 mabiguity by introducing auxiliary information. However,
 875 their focus diverges significantly from the present study, which
 876 is dedicated to resolving emotional ambiguity strictly within
 877 the speech modality. As such, methods that either ignore
 878 emotional ambiguity or introduce additional modalities are
 879 excluded from our comparisons.

880 The following models are included in our evaluation:

- 881 **Co-teaching (2021):** A progressive co-teaching frame-
 882 work that uses loss values to estimate sample difficulty,
 883 gradually training the model from simple to hard samples
 884 to mitigate issues with early-stage interference caused by
 885 emotionally ambiguous speech [30].
- 886 **Attention-LSTM-Attention (2020):** A SER model com-
 887 bining attention mechanisms and LSTMa to extract em-
 888 otional features across both temporal and feature dimen-
 889 sions. This approach constructs a derived dataset from
 890 IEMOCAP, distinguishing between clear and ambiguous
 891 samples to evaluate the dataset’s reliability and its impact
 892 on model performance [29].
- 893 **LLMs (2024):** A method that synthesizes emotionally
 894 rich speech data using large language models (LLMs)
 895 combined with IEMOCAP and student speech datasets.
 896 Transformer-based architectures are used for spatial fea-
 897 ture extraction to enhance data reliability. [28].
- 898 **Soft-target Training (2018):** A soft-label training
 899 method that adjusts soft label representations to effec-
 900 tively utilize ambiguous speech samples without domi-
 901 nant consensus labels [31].
- 902 **Inter-class Difference Loss (2023):** A multi-label train-
 903 ing approach that introduces an inter-class difference loss
 904 function that enabled the network to automatically learn
 905 the distribution of emotions by emphasizing differnces
 906 between emotion categories. [14].
- 907 **Emotion Existence (2019):** A method that first estimates
 908 the presence or absence of each emotion in speech sam-
 909 ples using multiple labels and then refines the estimates
 910 with soft labels to resolve emotional ambiguity [13].
- 911 **Meta-learning (2020):** A meta-learning framework that
 912 performs real-time correction of noisy labels and es-
 913 timates sample contribution weights, aiming to correct
 914 ambiguously labeled samples and reduce their negative
 915 impact during model training [34].
- 916 **AMSNet (2023):** A multi-scale attention-based frame-
 917 work designed to enhance the discriminative power of
 918 speech emotion representations. The framework employs
 919 segment-level feature refinement and hierarchical atten-
 920 tion to improve robustness against ambiguous emotional
 921 expressions [49].
- 922 **STACN (2025):** A sparse temporal aware capsule net-
 923 work designed to improve robustness against ambiguous
 924 or noisy emotional labels by integrating sparse temporal
 925 modeling, multi-head attention, and capsule-based feature
 926 routing, achieving stable performance in speech emotion
 927 recognition tasks [50].

TABLE III: **Comparison with the state-of-the-art.** The proposed model leads to the best overall performance both in terms of WA and UA.

Method	Label	Train set		Metrics	
		Clear	Ambiguous	WA (%)	UA (%)
Co-teaching (2021) [30]	Consensus	✓	-	62.3	-
Attention-LSTM (2020) [29]	Consensus	✓	✓	67.7	65.1
LLMs (2024) [28]	Consensus	✓	-	-	66.6
		✓	-	58.5	57.4
Soft-target (2018) [31]	Soft	-	✓	53.6	54.0
		✓	✓	62.6	63.7
		✓	-	66.0	63.9
Inter-class (2023) [14]	Multi	-	✓	60.5	61.7
		✓	✓	68.3	66.2
Emotion existence (2019) [13]	Multi & Soft	✓	✓	66.1	65.4
Meta-learning (2020) [34]	Update Consensus	✓	-	65.9	61.4
AMSNet (2023) [49]	Multi	✓	✓	69.2	70.5
STACN (2025) [50]	Multi	✓	✓	68.8	-
Proposed model (ours)	Update soft	✓	✓	70.3	71.3

E. Comparisons with State-Of-The-Art Methods

In the first set of experiments, we compare the proposed model with competing state-of-the-art (SOTA) SER models from the literature. We train our models on either clear, ambiguous or both types of samples (depending on the capabilities of the model), as detailed in Table III. To ensure a fair comparison, the results of other baseline methods are directly cited from the corresponding literature. From the presented results, it can be seen that the proposed model demonstrates superior performance over all considered methods in both weighted accuracy (WA) and unweighted accuracy (UA), achieving a WA score of 70.3% and UA score of 71.3.

SOTA Comparison. Compared to models that focus on enhancing dataset reliability or leveraging different feature representations, our method delivers consistent improvements. Specifically, relative to Attention-LSTM-Attention (2020) [29], we observe a 2.6% point gain in WA and a 6.2% point gain in UA. Compared to LLMs [28], our model achieves a 4.7% point improvement in UA. These results highlight that dataset augmentation alone does not sufficiently resolve the label noise caused by subjective annotation errors. In comparison to Co-teaching [30], we observe an 8.0% point increase in WA. This improvement can be attributed to our model’s ability to capture fine-grained spatial-temporal information through a dedicated network structure, as well as the dynamic adjustment of ambiguous labels during training.

When comparing to models that directly use observation labels of ambiguous speech without correction, our model also exhibits clear advantages. For instance, compared with Soft-target training [31], our approach improves WA and UA by 7.7% and 7.6% points, respectively. This is largely due to our real-time correction strategy, which reduces dependence on potentially inaccurate observation labels. Compared with Inter-class Difference Loss [14], we achieve 2.0% and 5.1% points improvements in WA and UA, respectively. These gains demonstrate the effectiveness of balancing the contributions of original soft labels and model-generated labels via the correction coefficient α .

In terms of label correction approaches, our model also

TABLE IV: **Performance statistics** across LOSO folds. Mean, standard deviation, and 95% confidence intervals are reported.

Metric	Mean (%)	Std (%)	95% CI (%)
WA	70.32	± 3.02	[68.16, 72.49]
UA	71.30	± 3.34	[68.91, 73.69]

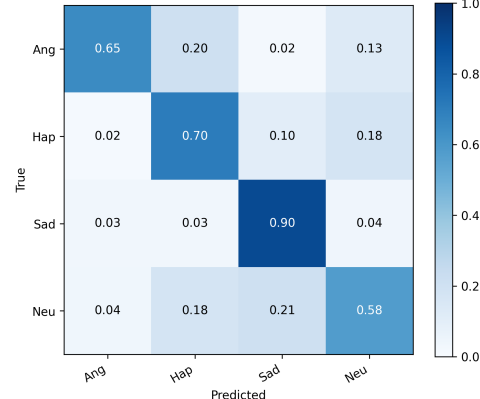


Fig. 5: **Confusion matrix** of the proposed model under one LOSO fold. The figure illustrates the per-class recognition performance, indicating that the model performs reliably across different categories, with noticeable confusions mainly between *Happiness/Sadness* and *Neutrality*.

967 outperforms existing methods. Compared to Emotion Existence [13], we observe improvements of 4.2% points in WA
968 and 5.9% points in UA. This suggests that our method better
969 captures the emotional nuances in speech samples lacking a
970 discrete consensus label. Similarly, when compared with Meta-
971 learning [34], our model shows substantial improvements, i.e.,
972 4.4% points in WA and 9.9% points in UA—due to its ability
973 to produce a smoother convergence path and to leverage a
974 broader set of ambiguous samples during training.
975

976 **Detailed Model Analysis.** To further assess the robustness of
977 the reported improvements over the state-of-the-art, Table IV
978 reports the mean, standard deviation, and 95% confidence
979 intervals across the 10 LOSO folds. Specifically, our model
980 achieves $WA = 70.32 \pm 3.02\%$ (95% CI: [68.16, 72.49]) and
981 $UA = 71.30 \pm 3.34\%$ (95% CI: [68.91, 73.69]), demonstrating
982 that the gains are consistent and statistically significant.
983

984 In addition to the standard WA and UA metrics, we also
985 report several supplementary indicators to provide a more
986 comprehensive assessment of the proposed model. These indi-
987 cators are summarized in Table V, which presents macro and
988 weighted versions of precision, recall, and F1-score. Together,
989 these metrics reflect class-balanced performance, robustness
990 under class imbalance, and the overall discriminative ability
991 of the model.

992 To further illustrate the per-class recognition performance,
993 we show in Fig. 5 the confusion matrix of the proposed
994 model under a randomly selected LOSO fold. The results
995 indicate that the model performs relatively consistently across
996 most categories, with noticeable confusions mainly between
997 *Happiness/Sadness* and *Neutrality*.

TABLE V: **Additional performance metrics of the proposed model.** To provide a more comprehensive evaluation as suggested by the reviewers, we report F1-score, weighted F1-score, macro/weighted precision, and macro/weighted recall of the proposed method.

Metric	Value (%)
F1-score (macro)	70.78
F1-score (weighted)	68.33
Precision (macro)	72.04
Precision (weighted)	70.97
Recall (macro)	71.59
Recall (weighted)	68.31

TABLE VI: **Inference efficiency of our model** measured on a single NVIDIA RTX 3090 GPU (batch size=1). Latency is averaged over 100 runs. RTF = real-time factor.

Input length (s)	FLOPs (G)	Latency (ms)	RTF	Peak Mem (GB)
1.00	6.95	4.44 ± 0.05	0.004	4.37
1.20	8.37	4.76 ± 0.02	0.004	4.39
1.60	11.21	5.16 ± 0.02	0.003	4.41
1.94	13.64	5.66 ± 0.04	0.003	4.45

F. Inference Efficiency

Beyond recognition accuracy, we also evaluate the inference efficiency of our model, as real-time performance is essential for HCI applications. Table VI summarizes the FLOPs, inference latency, real-time factor (RTF), and peak memory consumption across different input lengths. The RTF is simply obtained by dividing the inference time by the input audio duration. Our measurements show that the model achieves efficient inference with moderate GPU memory usage (~ 4.4 GB), demonstrating its suitability for practical deployment. It should be noted that publicly available code resources for related approaches are very limited, and most prior works do not report detailed efficiency statistics, which further highlights the contribution of our analysis.

G. Ablation Analysis

The comparative analysis presented in the previous section demonstrates that our proposed model outperforms existing approaches in handling ambiguous speech. In the next series of experiments, we conduct a series of ablation studies to better understand the impact of individual model components and learning objectives. While spatio-temporal models have been extensively explored in prior research, we focus our ablation studies on the main contributions of this, such as the real-time soft label correction module and associated learning objectives. Specifically, in the ablation studies, we explore: (i) the impact of the spatio-temporal network module, (ii) the influence of the soft label correction coefficient α and the margin control coefficient β , and (iii) the effect of different loss combinations in the overall learning objective.

Impact of the Spatio-Temporal Module. Table VII presents an analysis of the contributions of different architectural modules on the recognition performance of our model on the

TABLE VII: **Ablation study** exploring the impact of different model components, i.e., features used in the fusion module.

Fold	Impact analysis of multiple fusion modules							
	Spatial-only model		Temporal-only model		Spatial-temporal integrated model		Spatial-temporal multi-fusion model	
	WA (%)	UA (%)	WA (%)	UA (%)	WA (%)	UA (%)	WA (%)	UA (%)
1	45.1	44.0	70.3	70.4	68.6	69.9	69.6	71.0
2	51.1	55.2	66.3	66.7	68.4	68.6	69.8	70.9
3	44.6	44.9	69.0	72.8	68.8	73.1	73.0	75.5
4	54.3	53.2	73.4	73.4	70.7	70.1	74.6	76.2
5	50.1	49.9	64.8	64.7	64.3	64.9	66.7	67.6
6	48.8	47.3	66.8	66.2	68.0	67.5	68.6	68.1
7	39.5	35.8	62.9	64.0	62.6	63.5	65.4	66.6
8	46.6	49.5	70.5	70.0	69.6	70.0	73.7	72.7
9	47.8	50.4	68.9	69.4	70.2	69.8	69.7	70.0
10	38.1	41.8	70.1	71.4	70.8	70.6	72.2	74.4
Average	46.6	47.2	68.3	68.9	68.2	68.7	70.3	71.3

1029 IEMOCAP dataset. The results indicate that the spatial-only 1030 model performs significantly worse than other configurations, 1031 highlighting its inability to capture temporal dynamics, an 1032 essential component for emotion recognition. In contrast, the 1033 temporal-only model achieves performance closer to the full 1034 spatial-temporal model, suggesting that temporal features play 1035 a more dominant role in our overall framework. However, the 1036 best performance is observed with the spatial-temporal multi- 1037 fusion model, which leverages the complementary strengths of 1038 both spatial and temporal representations. This result confirms 1039 the effectiveness of jointly modeling spatial and temporal 1040 feature interactions for improved emotion classification.

1041 **Impact of Hyperparameters α and β .** Table VIII shows 1042 the influence of different correction coefficients α and margin 1043 control coefficients β on model training. To determine the 1044 optimal settings for these hyperparameters, we adopt a controlled 1045 variable approach by tuning one parameter at a time while 1046 holding the other constant. We begin by fixing $\beta = 0.1$ and 1047 varying α to observe its influence on performance. Results 1048 show that the model achieves the strongest performance when 1049 the value of α equals $\alpha = 0.3$.

1050 Subsequently, keeping $\alpha = 0.3$ fixed, we evaluate different 1051 values of β and find that $\beta = 0.1$ yields the highest performance. 1052 As shown in Table VIII, using $\alpha = 0.3$ and $\beta = 0.1$ 1053 results in 0.2% points improvement in both weighted accuracy 1054 (WA) and unweighted accuracy (UA) compared to using $\alpha = 0$ 1055 with the same β . This performance gain is attributed to the 1056 presence of noise in the observation labels of ambiguous 1057 speech, and the ability of α to balance the influence between 1058 observed and model-generated labels. Additionally, we see that 1059 setting $\alpha = 0$ disables the online correction process and forces 1060 the model to rely solely on static soft labels. As shown in 1061 Table VIII, this leads to a drop in both weighted accuracy 1062 (WA) and unweighted accuracy (UA), indicating that updating 1063 of ambiguous labels in real-time contributes positively to the 1064 overall performance. This confirms that the iterative, online 1065 correction mechanism plays an essential role in mitigating the 1066 impact of annotation ambiguity. Furthermore, we observe that 1067 increasing β beyond 0.1 (with $\alpha = 0.3$) leads to a decline in 1068 model performance. This is likely because an excessively large 1069 margin coefficient suppresses valuable prediction signals from

TABLE VIII: **Sensitivity analysis** with respect to the correction coefficient α and margin control coefficient β .

$\alpha(\beta = 0.1)$	WA (%)	UA (%)	$\beta(\alpha = 0.3)$	WA (%)	UA (%)
0	69.5	70.6	0	69.8	71.0
0.1	69.8	71.0	0.1	70.3	71.3
0.2	69.8	70.1	0.2	70.0	70.7
0.3	70.3	71.3	0.3	69.6	70.4
0.4	69.8	71.1	0.4	69.5	70.7
0.5	69.7	70.9	0.5	69.7	70.7
0.6	69.5	70.9	0.6	69.3	70.2
0.7	70.0	70.7	0.7	69.3	70.6
0.8	69.6	70.9	0.8	69.4	70.3
0.9	69.4	70.6	0.9	69.2	70.5

emotion-positive categories, thereby reducing the effectiveness 1070 of the correction mechanism. 1071

1072 **Impact of Loss Functions.** Table IX presents an analysis 1073 of model performance under different combinations of loss 1074 functions. To ensure consistency and fairness in the ablation 1075 experiments, we fix the correction coefficient to $\alpha = 0.3$ and 1076 the margin control coefficient to $\beta = 0.1$. Additionally, Fig. 6 1077 provides t-SNE visualizations, illustrating the distribution of 1078 emotional features learned under each loss configuration. 1079

1080 From the results in Table IX, we observe that both the cross- 1081 entropy loss L_{cor} and the enhanced inter-class difference loss 1082 L_{Ic} contribute most effectively when used in their respective 1083 roles, i.e., L_{cor} as the primary loss function for training on 1084 clear speech samples, and L_{Ic} as a regularization term for 1085 correcting soft labels in ambiguous samples. Compared to 1086 using either L_{cor} or L_{Ic} alone for both training and correction, 1087 the combined loss function improves weighted accuracy (WA) 1088 by 0.1% and 0.7% points, and unweighted accuracy (UA) by 1089 0.3% and 0.9% points, respectively. 1090

1091 These results can be attributed to the complementary nature 1092 of the two loss functions. While L_{cor} is well-suited for optim- 1093 izing predictions on clearly labeled data, it lacks the ability 1094 to effectively handle ambiguity in soft labels. In contrast, L_{Ic} 1095 is designed to increase inter-class separability in emotionally 1096 ambiguous samples but provides limited benefit for already 1097 well-separated clear samples. As previously observed in Ta- 1098 ble VIII, excessively increasing the boundary margin via β can 1099 actually degrade performance, particularly on clear samples 1100 where emotional boundaries are already well-defined. Thus, 1101 employing a hybrid loss function that combines both L_{cor} and 1102 L_{Ic} allows the model to capitalize on the strengths of each: 1103 robust learning from clear data and improved label correction 1104 for ambiguous cases. 1105

1106 **t-SNE Visualizations.** Figure 6 presents a t-SNE visualization 1107 of the learned emotion representations under the four training 1108 configurations. As can be seen, the degree of emotional 1109 clustering follows the pattern: (c) > (a) > (b) > (d). This 1110 pattern highlights the effectiveness of the soft label correction 1111 strategy in mitigating the negative impact of label noise in 1112 ambiguous speech, which otherwise misguides model training. 1113

1114 A closer comparison between subfigures (c) and (a) reveals 1115

TABLE IX: **Ablation study** with respect to the components of the overall learning objective.

Fold	L_{cor} and L_{cor}		L_{Ic} and L_{Ic}		L_{cor} and L_{Ic}	
	WA (%)	UA (%)	WA (%)	UA (%)	WA (%)	UA (%)
1	70.4	70.7	69.0	70.3	69.6	71.0
2	68.5	70.1	68.7	69.5	69.8	70.9
3	71.5	75.3	71.2	74.8	73.0	75.5
4	74.3	75.4	70.5	71.8	74.6	76.2
5	66.7	67.2	65.2	65.8	66.7	67.6
6	67.7	65.9	70.3	69.6	68.6	68.1
7	65.0	67.6	65.9	67.4	65.4	66.6
8	74.9	72.4	73.0	71.1	73.7	72.7
9	70.5	71.3	71.7	70.7	69.7	70.0
10	72.2	74.5	70.5	72.6	72.2	74.4
Average	70.2	71.0	69.6	70.4	70.3	71.3

that emotion clusters in (a) are more scattered and distributed in four distinct directions, consistent with the results in Table IX. This observation supports the conclusion that the cross-entropy loss function alone lacks sufficient discriminative power for ambiguous emotion categories. Further comparisons between (c) and (b) show that although (b) exhibits a larger inter-class margin, the distribution of neutral emotions is more diffuse and significantly overlaps with other categories. This suggests that while L_{Ic} effectively increases inter-class separation, it can simultaneously introduce confusion—particularly for more ambiguous emotion types such as neutrality. Lastly, in comparing (c) and (d), we observe that the clusters corresponding to happiness, anger, and neutral emotions in (c) are more compact and well-separated. This demonstrates that soft label correction on ambiguous speech samples helps guide the model to better capture the underlying emotional distribution.

VI. SUMMARY

In this paper, we proposed an enhanced ambiguous speech emotion recognition model to address several key challenges in the field: the over-reliance on subjectively annotated labels, the disregard for proportional differences among emotions within multi-label annotations, and the underutilization of speech samples lacking dominant consensus labels. Our model integrates Convolutional Neural Networks (CNN) and Wav2Vec 2.0 to jointly capture spatial and temporal characteristics of speech, with a multi-level fusion mechanism that adaptively balances these features for more effective representation. A key contribution of the proposed approach is the introduction of a real-time soft label correction strategy, specifically designed to handle ambiguous labels by dynamically refining them during training. This helps reduce the adverse effects of noisy annotations on model convergence. This novel real-time refinement mechanism distinguishes our approach from existing soft-label or offline correction approaches, thereby strengthening the overall novelty of our method. We also provided a formal mathematical proof of the feasibility and effectiveness of the proposed correction mechanism. Extensive experiments conducted on the IEMOCAP dataset confirmed the superiority of our method, yielding improvements of 2.0%

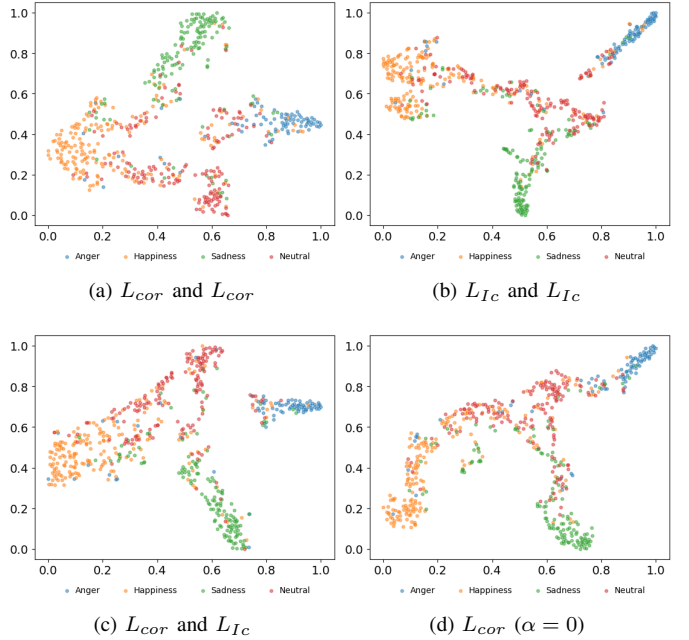


Fig. 6: **t-SNE plots for different loss combinations** with $\alpha = 0.3, \beta = 0.1$: (a) L_{cor} is used for both model training and soft label correction; (b) Enhanced L_{Ic} is used for both model training and soft label correction; (c) Enhanced L_{Ic} is used for soft label correction and L_{cor} is used for model training; (d) No soft label correction is applied ($\alpha = 0$), L_{cor} is used for training, and β is unrestricted.

points in weighted accuracy (WA) and 4.7% in unweighted accuracy (UA) over existing state-of-the-art approaches. Furthermore, ablation studies on the real-time soft label correction module highlighted its critical role in enhancing model performance and provided deeper insights into its contribution.

REFERENCES

- [1] B. W. Schuller, “Speech emotion recognition: Two decades in a nutshell, benchmarks, and ongoing trends,” *Communications of the ACM*, vol. 61, no. 5, pp. 90–99, 2018.
- [2] M. Gerczuk, S. Amiriparian, S. Ottl, and B. W. Schuller, “Emonet: A transfer learning framework for multi-corpus speech emotion recognition,” *IEEE Transactions on Affective Computing*, vol. 14, no. 2, pp. 1472–1487, 2021.
- [3] S. Shen, F. Liu, H. Wang, and A. Zhou, “Towards speaker-unknown emotion recognition in conversation via progressive contrastive deep supervision,” *IEEE Transactions on Affective Computing*, 2025.
- [4] M. S. Hossain and G. Muhammad, “Emotion recognition using deep learning approach from audio-visual emotional big data,” *Information Fusion*, vol. 49, pp. 69–78, 2019.
- [5] W. Zhu and X. Li, “Speech emotion recognition with global-aware fusion on multi-scale feature representation,” in *ICASSP 2022-2022 IEEE International Conference on Acoustics, Speech and Signal Processing (ICASSP)*. IEEE, 2022, pp. 6437–6441.
- [6] A. B. Nassif, I. Shahin, I. Attili, M. Azzeh, and K. Shaalan, “Speech recognition using deep neural networks: A systematic review,” *IEEE access*, vol. 7, pp. 19 143–19 165, 2019.
- [7] M. Hou, Z. Zhang, Q. Cao, D. Zhang, and G. Lu, “Multi-view speech emotion recognition via collective relation construction,” *IEEE/ACM Transactions on Audio, Speech, and Language Processing*, vol. 30, pp. 218–229, 2021.
- [8] W. Fan, X. Xu, B. Cai, and X. Xing, “Isnet: Individual standardization network for speech emotion recognition,” *IEEE/ACM Transactions on Audio, Speech, and Language Processing*, vol. 30, pp. 1803–1814, 2022.

[9] Y. Kim and J. Kim, "Human-like emotion recognition: Multi-label learning from noisy labeled audio-visual expressive speech," in *2018 IEEE International Conference on Acoustics, Speech and Signal Processing (ICASSP)*. IEEE, 2018, pp. 5104–5108.

[10] R. Lotfian and C. Busso, "Curriculum learning for speech emotion recognition from crowdsourced labels," *IEEE/ACM Transactions on Audio, Speech, and Language Processing*, vol. 27, no. 4, pp. 815–826, 2019.

[11] H. M. Fayek, M. Lech, and L. Cavedon, "Modeling subjectiveness in emotion recognition with deep neural networks: Ensembles vs soft labels," in *2016 international joint conference on neural networks (IJCNN)*. IEEE, 2016, pp. 566–570.

[12] M. Lukasik, S. Bhojanapalli, A. Menon, and S. Kumar, "Does label smoothing mitigate label noise?" in *International Conference on Machine Learning*. PMLR, 2020, pp. 6448–6458.

[13] A. Ando, R. Masumura, H. Kamiyama, S. Kobashikawa, and Y. Aono, "Speech emotion recognition based on multi-label emotion existence model," in *INTERSPEECH*, 2019, pp. 2818–2822.

[14] X. Li, Z. Zhang, C. Gan, and Y. Xiang, "Multi-label speech emotion recognition via inter-class difference loss under response residual network," *IEEE Transactions on Multimedia*, vol. 25, pp. 1520–9210, 2023.

[15] S. Steidl, M. Levit, A. Batliner, E. Noth, and H. Niemann, "“of all things the measure is man” automatic classification of emotions and inter-labeler consistency [speech-based emotion recognition]," in *Proceedings. (ICASSP’05). IEEE International Conference on Acoustics, Speech, and Signal Processing, 2005*, vol. 1. IEEE, 2005, pp. I–317.

[16] S. Mao, P. Ching, and T. Lee, "Enhancing segment-based speech emotion recognition by iterative self-learning," *IEEE/ACM Transactions on Audio, Speech, and Language Processing*, vol. 30, pp. 123–134, 2021.

[17] Y. Zhou, X. Liang, Y. Gu, Y. Yin, and L. Yao, "Multi-classifier interactive learning for ambiguous speech emotion recognition," *IEEE/ACM transactions on audio, speech, and language processing*, vol. 30, pp. 695–705, 2022.

[18] H.-C. Chou and C.-C. Lee, "Every rating matters: Joint learning of subjective labels and individual annotators for speech emotion classification," in *ICASSP 2019-2019 IEEE International Conference on Acoustics, Speech and Signal Processing (ICASSP)*. IEEE, 2019, pp. 5886–5890.

[19] H.-C. Chou, L. Goncalves, S.-G. Leem, A. N. Salman, C.-C. Lee, and C. Busso, "Minority views matter: Evaluating speech emotion classifiers with human subjective annotations by an all-inclusive aggregation rule," *IEEE Transactions on Affective Computing*, 2024.

[20] S. Latif, R. Rana, S. Khalifa, R. Jurdak, J. Qadir, and B. Schuller, "Survey of deep representation learning for speech emotion recognition," *IEEE Transactions on Affective Computing*, vol. 14, no. 2, pp. 1634–1654, 2021.

[21] T. M. Wani, T. S. Gunawan, S. A. A. Qadri, M. Kartiwi, and E. Ambikairajah, "A comprehensive review of speech emotion recognition systems," *IEEE Access*, vol. 9, pp. 47 795–47 814, 2021.

[22] A. Hashem, M. Arif, and M. Alghamdi, "Speech emotion recognition approaches: A systematic review," *Speech Communication*, vol. 154, p. 102974, 2023.

[23] S. M. George and P. M. Ilyas, "A review on speech emotion recognition: a survey, recent advances, challenges, and the influence of noise," *Neurocomputing*, vol. 568, p. 127015, 2024.

[24] J. Ye, X.-C. Wen, Y. Wei, Y. Xu, K. Liu, and H. Shan, "Temporal modeling matters: A novel temporal emotional modeling approach for speech emotion recognition," in *ICASSP 2023-2023 IEEE International Conference on Acoustics, Speech and Signal Processing (ICASSP)*. IEEE, 2023, pp. 1–5.

[25] S. Li, X. Xing, W. Fan, B. Cai, P. Fordson, and X. Xu, "Spatiotemporal and frequentional cascaded attention networks for speech emotion recognition," *Neurocomputing*, vol. 448, pp. 238–248, 2021.

[26] X. Wu, Y. Cao, H. Lu, S. Liu, D. Wang, Z. Wu, X. Liu, and H. Meng, "Speech emotion recognition using sequential capsule networks," *IEEE/ACM Transactions on Audio, Speech, and Language Processing*, vol. 29, pp. 3280–3291, 2021.

[27] C. Gan, K. Wang, Q. Zhu, Y. Xiang, D. K. Jain, and S. García, "Speech emotion recognition via multiple fusion under spatial-temporal parallel network," *Neurocomputing*, vol. 555, p. 126623, 2023.

[28] L. Wang, J. Yang, Y. Wang, Y. Qi, S. Wang, and J. Li, "Integrating large language models (llms) and deep representations of emotional features for the recognition and evaluation of emotions in spoken english," *Applied Sciences*, vol. 14, no. 9, p. 3543, 2024.

[29] Y. Yu and Y.-J. Kim, "Attention-lstm-attention model for speech emotion recognition and analysis of iemocap database," *Electronics*, vol. 9, no. 5, p. 713, 2020.

[30] Y. Yin, Y. Gu, L. Yao, Y. Zhou, X. Liang, and H. Zhang, "Progressive co-teaching for ambiguous speech emotion recognition," in *ICASSP 2021-2021 IEEE International Conference on Acoustics, Speech and Signal Processing (ICASSP)*. IEEE, 2021, pp. 6264–6268.

[31] A. Ando, S. Kobashikawa, H. Kamiyama, R. Masumura, Y. Ijima, and Y. Aono, "Soft-target training with ambiguous emotional utterances for dnn-based speech emotion classification," in *2018 IEEE International Conference on Acoustics, Speech and Signal Processing (ICASSP)*. IEEE, 2018, pp. 4964–4968.

[32] C. Wang, J. Shi, C. Tao, F. Xu, X. Tang, L. Li, Y. Zhou, B. Tian, S. Wei, and X. Zhang, "Multitype label noise modeling and uncertainty-weighted label correction for concealed object detection," *IEEE Transactions on Instrumentation and Measurement*, vol. 72, pp. 1–12, 2023.

[33] D. Liu, I. W. Tsang, and G. Yang, "A convergence path to deep learning on noisy labels," *IEEE Transactions on Neural Networks and Learning Systems*, vol. 33, no. 4, pp. 5170–5182, 2022.

[34] T. Fujioka, T. Homma, and K. Nagamatsu, "Meta-learning for speech emotion recognition considering ambiguity of emotion labels," in *INTERSPEECH*, 2020, pp. 2332–2336.

[35] S. Mao, P.-C. Ching, and T. Lee, "Emotion profile refinery for speech emotion classification," *INTERSPEECH*, pp. 531–535, 2020.

[36] Y. Yin, Y. Gu, L. Yao, Y. Zhou, X. Liang, and H. Zhang, "Progressive co-teaching for ambiguous speech emotion recognition," in *ICASSP 2021-2021 IEEE International Conference on Acoustics, Speech and Signal Processing (ICASSP)*. IEEE, 2021, pp. 6264–6268.

[37] S. Chopra, P. Mathur, R. Sawhney, and R. R. Shah, "Meta-learning for low-resource speech emotion recognition," in *ICASSP 2021-2021 IEEE International Conference on Acoustics, Speech and Signal Processing (ICASSP)*. IEEE, 2021, pp. 6259–6263.

[38] R. Cai, K. Guo, B. Xu, X. Yang, and Z. Zhang, "Meta multi-task learning for speech emotion recognition," in *Interspeech*, 2020, pp. 3336–3340.

[39] C. Zhang, S. Bengio, M. Hardt, B. Recht, and O. Vinyals, "Understanding deep learning (still) requires rethinking generalization," *Communications of the ACM*, vol. 64, no. 3, pp. 107–115, 2021.

[40] G. Li, J. Hou, Y. Liu, and J. Wei, "Mvib-dva: Learning minimum sufficient multi-feature speech emotion embeddings under dual-view aware," *Expert Systems with Applications*, vol. 246, p. 123110, 2024.

[41] A. Derington, H. Wierstorf, A. Özkil, F. Ebyen, F. Burkhardt, and B. W. Schuller, "Testing correctness, fairness, and robustness of speech emotion recognition models," *IEEE Transactions on Affective Computing*, 2025.

[42] C. Busso, M. Bulut, C.-C. Lee, A. Kazemzadeh, E. Mower, S. Kim, J. N. Chang, S. Lee, and S. S. Narayanan, "Iemocap: Interactive emotional dyadic motion capture database," *Language resources and evaluation*, vol. 42, no. 4, pp. 335–359, 2008.

[43] A. Aftab, A. Morsali, S. Ghaemmaghami, and B. Champagne, "Light-ssnet: A lightweight fully convolutional neural network for speech emotion recognition," in *ICASSP 2022-2022 IEEE international conference on acoustics, speech and signal processing (ICASSP)*. IEEE, 2022, pp. 6912–6916.

[44] M. Chen, X. He, J. Yang, and H. Zhang, "3-d convolutional recurrent neural networks with attention model for speech emotion recognition," *IEEE Signal Processing Letters*, vol. 25, no. 10, pp. 1440–1444, 2018.

[45] Q. Cao, M. Hou, B. Chen, Z. Zhang, and G. Lu, "Hierarchical network based on the fusion of static and dynamic features for speech emotion recognition," in *ICASSP 2021-2021 IEEE International Conference on Acoustics, Speech and Signal Processing (ICASSP)*. IEEE, 2021, pp. 6334–6338.

[46] Y. Wang, A. Boumadane, and A. Heba, "A fine-tuned wav2vec 2.0/hubert benchmark for speech emotion recognition, speaker verification and spoken language understanding," *arXiv preprint arXiv:2111.02735*, 2021.

[47] Y. Song and Q. Zhou, "Bi-modal bi-task emotion recognition based on transformer architecture," *Applied Artificial Intelligence*, vol. 38, no. 1, p. 2356992, 2024.

[48] B. T. Atmaja, K. Shirai, and M. Akagi, "Speech emotion recognition using speech feature and word embedding," in *2019 Asia-Pacific Signal and Information Processing Association Annual Summit and Conference (APSIPA ASC)*. IEEE, 2019, pp. 519–523.

[49] Z. Chen, J. Li, H. Liu, X. Wang, H. Wang, and Q. Zheng, "Learning multi-scale features for speech emotion recognition with connection attention mechanism," *Expert Systems with Applications*, vol. 214, p. 118943, 2023.

[50] H. Zhang, H. Huang, P. Zhao, and Z. Yu, "Sparse temporal aware capsule network for robust speech emotion recognition," *Engineering Applications of Artificial Intelligence*, vol. 144, p. 110060, 2025.



1335
1336
1337
1338
1339
1340
1341
1342
1343
Chenquan Gan received the Ph.D. degree from the Department of Computer Science, Chongqing University, Chongqing, China, in 2015. He is currently an Associate Professor with Chongqing University of Post and Telecommunications (CQUPT), Chongqing. His research interests include network propagation and control, sentiment analysis, and blockchain.



1344
1345
1346
1347
1348
Daitao Zhou is currently pursuing the M.S. degree with the Chongqing University of Posts and Telecommunications, Chongqing, China. His research interests is sentiment analysis.



1349
1350
1351
1352
1353
1354
1355
1356
1357
1358
1359
Qingyi Zhu received the Ph.D. degree in computer science and technology from the College of Computer Science, Chongqing University, Chongqing, China, in 2014. He is currently a Professor with the Chongqing University of Posts and Telecommunications, Chongqing. He has published more than 60 academic articles in peer-reviewed international journals. His current research interests include cybersecurity dynamics, complex systems, and blockchain.



1360
1361
1362
1363
1364
1365
1366
Xibin Wang received a PhD degree in computer science from Chongqing University in 2015. He is a professor and vice dean in the School of Data Science at Guizhou Institute of Technology. His research interests include recommendation systems, data mining and service computing.



1367
1368
1369
1370
1371
1372
1373
1374
1375
1376
1377
Deepak Kumar Jain (Senior Member, IEEE) received the Ph.D. degree in pattern recognition and intelligent system from the Institute of Automation, University of Chinese Academy of Sciences, Beijing, China, in 2018. He is currently an Associate Professor with Dalian University of Technology, Dalian, China. He has presented several papers in peer-reviewed conferences and has authored or co-authored numerous studies in science cited journals. His research interests include deep learning, machine learning, pattern recognition, and computer vision.



1378
1379
1380
1381
1382
1383
1384
1385
1386
1387
1388
Vitomir Štruc is a Full Professor at the University of Ljubljana, Slovenia, and an expert on computer vision and machine learning. He has co-authored over 200 papers in leading international journals and conferences. Vitomir serves as Deputy Editor-in-Chief of IEEE T-IFS, Subject Editor for Signal Processing, and Associate Editor for Pattern Recognition. Dr. Štruc is a Senior IEEE member, current VP Technical Activities of the IEEE Biometrics Council, the secretary of IAPR TC4, and a supervisory board member of the EAB.